PCP
PLANT & CELL PHYSIOLOGY

Characterization of Target Site of Aluminum Phytotoxicity in Photosynthetic Electron Transport by Fluorescence Techniques in Tobacco Leaves

Zhe Li, Fuqiang Xing and Da Xing*

MOE Key Laboratory of Laser Life Science & Institute of Laser Life Science, College of Biophotonics, South China Normal University, Guangzhou 510631, China

*Corresponding author: Email, xingda@scnu.edu.cn; Fax, +86-20-8521-6052.

(Received December 9, 2011; Accepted May 12, 2012)

Regular Paper

Aluminum (Al) toxicity limits crop yield in acidic soil through affecting diverse metabolic processes, especially photosynthesis. The aim of this work was to examine the effect of Al on photosynthetic electron transport in vivo as determined by chlorophyll fluorescence and delayed fluorescence of tobacco leaves. Results showed that Al treatment inhibited the photosynthetic rate and electron transfer, and decreased photosystem (PS) II photochemical activity in a time- and concentration-dependent manner, which could not be obviously alleviated by the addition of the reactive oxygen species (ROS) scavenger ascorbic acid (AsA). These results suggested that photosynthetic electron transfer chain components, especially PSII, might be directly damaged by Al instead of in an ROS-dependent manner. Furthermore, the fluorescence imaging and biochemical analysis exhibited that Al, after entering the cells, could accumulate in the chloroplasts, which paralleled the decreased content of Fe in the chloroplast. The changes in the chlorophyll fluorescence decay curve, the delayed fluorescence decay curve and the chlorophyll fluorescence parameters indicated that Al, through interacting with or replacing the non-heme iron between Q_A and Q_B, caused the inhibition of electron transfer between Q_A and Q_B, resulting in PSII photochemical damage and inhibition of the photosynthetic rate. In summary, our results characterized the target site of Al phytotoxicity in photosynthetic electron transport, providing new insight into the mechanism of Al phytotoxicity-induced chloroplast dysfunction and photosynthetic damage.

Keywords: Aluminum • Chlorophyll fluorescence • Delayed fluorescence • Photosystem II • Target sites • Tobacco.

Abbreviations: AAS, atomic absorption spectroscopy; Al, Aluminum; AsA, ascorbic acid; DCF, dichlorodihydrofluorescein; DF, delayed fluorescence; ETR, relative rate of photosynthetic electron transport; H_2DCFDA, 2′,7′-dichlorodihydrofluorescein diacetate; LCSM, laser confocal scanning microscope; PAR, photosynthetically active radiation; PMS, phenazine methosulfate; Pn, net photosynthetic rate; PS, photosystem; ROS, reactive oxygen species; SPCM, single-photon counting module.

Introduction

Aluminum (Al), as a non-essential metal widespread in the environment, is known to be toxic to humans as well as plants, causing damage to not only the root that is always exposed to Al but also to the aerial part of plants. A number of intracellular targets of Al have been identified, including the plasma membrane, mitochondria, peroxisomes and chloroplasts (Akaya and Takenaka 2001; Yamamoto et al. 2002; Chen et al. 2005; Li and Xing 2011). Its toxicity has been recognized as one of the major factors that limit crop production on acid soil through negatively affecting the nutrient uptake and diverse metabolic processes, especially photosynthesis (Moustakas et al. 1995; Ono et al. 1995; Chen et al. 2005; Mihailovic et al. 2008). Previous findings suggest that Al stress causes retarded growth and subsequent wilt by inducing chlorophyll degradation and decreasing the net photosynthetic rate (Pn) (Akaya and Takenaka 2001; Chen et al. 2005). It has also been found that Al decreases the amount of Rubisco activase and the β-subunit of the Rubisco subunit-binding protein in an oxidative burst-dependent manner (Moustakas et al. 1995; Akaya and Takenaka 2001).

Photosystem (PS) II, as the most sensitive component of the photosynthetic apparatus, is considered to play key roles in the photosynthetic response to environmental perturbations (Lu and Zhang 2000; Appenroth et al. 2001; Lu et al. 2003; Farage et al. 2006; Van Heerden et al. 2007; Ehlert and Hincha 2008; Zhao et al. 2008). Within the PSII complex, several targets have been suggested to be sensitive to various stresses and stimuli, including the residues of D1 protein (Sanakis et al. 1997; Wodala et al. 2008) and the non-heme iron (II) between Q_A and Q_B binding sites (Diner and Petrouleas 1990; Wodala et al. 2008). D1 protein is considered to be the PSII reaction center and has been shown to be sensitive to environmental stress conditions: various unfavorable conditions, such as drought, nutrient

Plant Cell Physiol. 53(7): 1295–1309 (2012) doi:10.1093/pcp/pcs076, available online at www.pcp.oxfordjournals.org

deficiency, heat, chemical stress, ozone fumigation as well as UV-B and visible light stresses, can influence the turnover of D1 protein (Giardi et al. 1997; Putty-Reddy et al. 2005). The terminal electron acceptor in PSII is the linear $Q_AFe^{2+}Q_B$ complex, which can accept the electron from the PSII reaction center. The rate of electron transfer between the two quinones (Q_A and Q_B) depends on the coordinative properties of the non-heme iron (II) that, under normal circumstances, forms coordinate covalent bonds with four His residues provided by the D1 and D2 reaction center subunits (Petrouleas and Diner 1990; Kern et al. 2005; Wodala et al. 2008). The herbicide DCMU can bind to Q_B, and other small molecules such as NO, CN^- and fluoride anions can reversibly bind to the non-heme iron (II) (Goussias et al. 2002), to inhibit the linear electron transfer. Previous studies have associated Al stress with an impaired PSII, including a reduction in the PSII electron transport rate and the closure of PSII reaction centers (Chen et al. 2005; Jiang et al. 2008). Though PSII has been recognized as an important site of action for Al, how PSII photochemical activity is affected by Al has not been thoroughly studied.

The aim of this work is to investigate the mechanism of how Al affects PSII photochemical activity and to characterize the target site of Al in the photosynthetic electron transport chain, in order to provide new insight into the mechanism of Al phytotoxicity-induced chloroplast dysfunction and photosynthetic damage.

Results

Treatment with Al leads to decreased photosynthetic capacity in tobacco leaves

Previous studies by our group demonstrate that delayed fluorescence (DF) and altered Pn values can accurately reflect photosynthetic damage under adverse stresses (Zhang and Xing 2008). DF, which is mainly emitted from PSII through inverse photochemical reactions, is an intrinsic label of the efficiency of charge separation at P680 (Zhang and Xing 2008). Pn, which is quantified by measuring rates of CO_2 consumption, can reflect the efficiency of CO_2 fixation (Wang et al. 2007). Hence, DF and Pn values were measured under Al treatment. The results showed that both DF and Pn exhibited a time- and concentration-dependent decrease (**Fig. 1A, B**), indicating the induction of photosynthetic damage by Al.

As parallel experiments, the electron transport capacity was investigated under Al stress. Light-response curves were measured to determine the relative electron transport rate (ETR). In **Fig. 2**, the light-response curves of ETR were compared for leaves treated with different concentrations of Al at the indicated times. With photosynthetically active radiation (PAR) ranging from 0 to 900 μmol quanta m^{-2} s^{-1}, the ETR values of leaves treated with different concentrations of Al (0.1 mM, 0.5 mM and 1 mM) all decreased comparing with the untreated control at 4, 8 and 12 h, and the decline was exhibited in a concentration- and time-dependent manner (**Fig. 2A–C**).

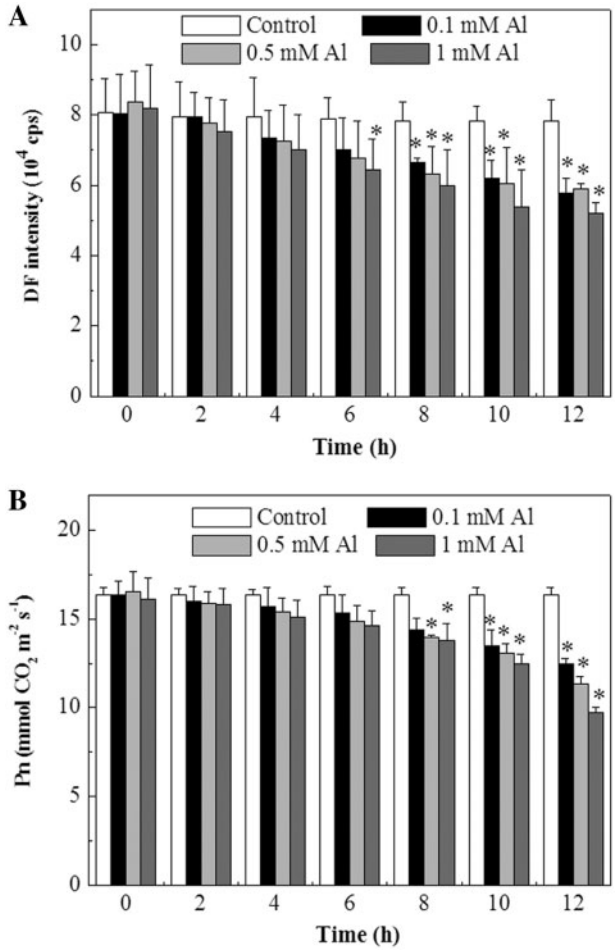

Fig. 1 Quantitative analysis of photosynthetic damage induced by Al. (A) Changes of DF in a time- and concentration-dependent manner. (B) Changes of Pn in a time- and concentration-dependent manner. Data are means ± SD of six independent experiments. Asterisks indicate a significant difference from the control at $P < 0.05$ by *t*-test.

While our results support the finding that Al has concentration- and time-dependent effects on photosynthesis, they reveal the importance of a certain 'light pressure' for the assessment of differences in the photosynthetic electron transport capacity between control and treated leaves, as well as between the samples treated with different Al concentrations. At PAR values <50 μmol quanta m^{-2} s^{-1}, under which the electron flow was limited by the light, there was almost no difference in ETR values between untreated and treated leaves, as well as between leaves treated with different Al concentrations. Moreover, with increasing PAR values, differences in the ETR values between the control and treated samples became increasingly evident (**Fig. 2**).

Changes of PSII and PSI activities under Al treatment

Chloroplasts are capable of light-induced charge separation, electron transfer from PSII to PSI, water photolysis and

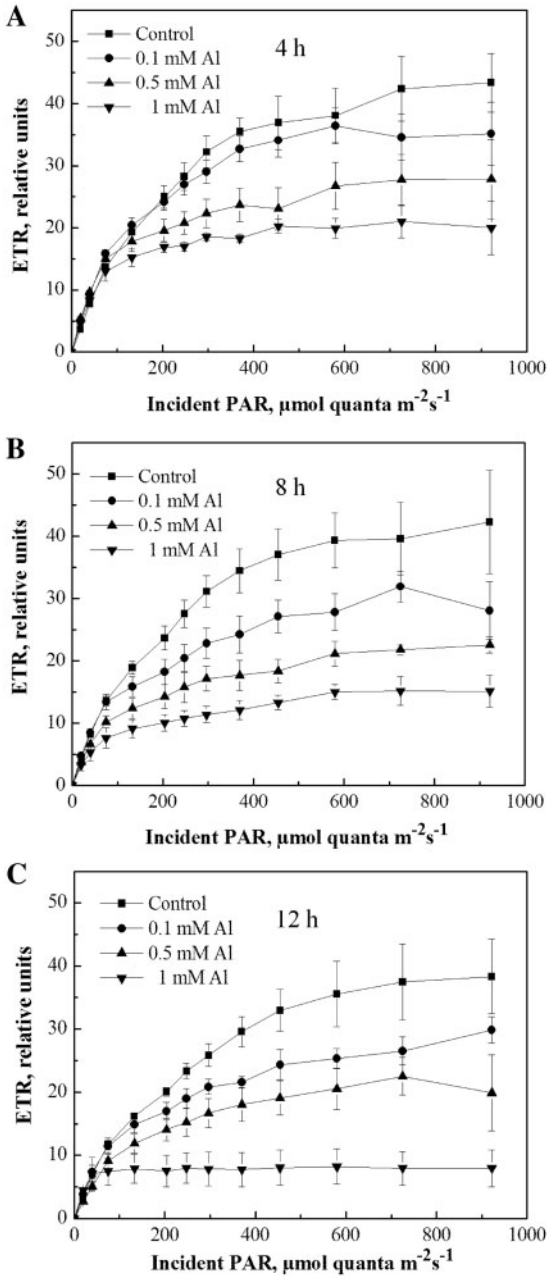

Fig. 2 Effects of Al on light-response curves of the relative photosynthetic electron transport rate (ETR). Leaves treated with Al were analyzed at 4 h (A), 8 h (B) and 12 h (C). Data are means ± SD of six independent experiments.

oxygen evolution. Hence, the effects of Al treatment on the activities of the two PSs were investigated using an oxygen electrode. Our results showed that under Al stress PSII activity exhibited a time- and concentration-dependent decrease, while PSI activity exhibited no obvious changes (**Fig. 3A, B**). At 8 h of 0.5 mM Al treatment, PSII activity decreased by about 33 ± 6% ($P < 0.05$) compared with that of control samples, and then decreased by about 69 ± 8% ($P < 0.05$) at 12 h of 0.5 mM Al treatment (**Fig. 3A**). For further confirmation, altered photophosphorylation rates were detected under Al treatment. Non-cyclic photophosphorylation requires that both of the two PSs are excited. The electron transport pathway of non-cyclic photophosphorylation is that an electron derived from water photolysis transfers through PSI, PSII and a succession of electron carriers before it transfers to $NADP^+$, which is eventually reduced to NADPH (Huang et al. 2008). Cyclic photophosphorylation occurs when only PSI is excited but PSII is not. During cyclic photophosphorylation, no photolysis of water occurs and therefore no reduced NADPH is produced (Huang et al. 2008). Our data showed that Al treatment apparently decreased the rate of non-cyclic photophosphorylation in a time- and concentration-dependent manner, but exerted no obvious effect on the rate of cyclic photophosphorylation (**Fig. 3C, D**), suggesting that Al treatment might mainly damage PSII activity. These results indicate that compared with PSI, PSII was the sensitive and major site damaged by Al toxicity in the photosynthetic electron transfer chain.

Characterization of PSII photochemical damage caused by Al treatment

In order to further characterize the mechanism of photosynthetic dysfunction caused by Al, the photochemical activity of PSII was investigated using chlorophyll fluorescence. The fluorescence parameters Fv/Fm (the maximum PSII quantum yield) and Y (II) (the effective PSII quantum yield), which represent the capacity for the photon energy absorbed by PSII to be utilized in photochemistry under dark- and light-adapted conditions, respectively (Chaerle and Van Der Straeten 2000; Baker and Rosenqvist 2004), were analyzed with Al-treated tobacco leaves. Distinct effects of different concentrations of Al on both of the two parameters were obvious in the treatment period of 12 h (**Figs. 3E, F**, **S1A**). At 4 h, changes in the photosynthetic parameters began to occur in leaves treated with 0.5 or 1 mM Al in contrast to those exposed to 0.1 mM Al, in which no changes could be detected. After 6-h treatment, all samples exhibited obvious changes in the false images of Fv/Fm and Y (II), but the degree and area differed according to the Al concentration (0.1–1 mM) (**Fig. S1A**). To statistically evaluate the data derived from the imaging experiments, the fluorescence parameters of leaves incubated with three different amounts of Al (0.1 mM, 0.5 mM and 1 mM) were assessed every 2 h during the treated period of 12 h. The results showed that the decrease in Fv/Fm was time and concentration dependent. As shown in **Fig. 3E**, Fv/Fm of leaves exposed to 0.1 mM Al did not vary from the levels expected for plants under non-stressed conditions (~0.800) until late in the course of treatment, in which a slight decline (to 0.650~0.700) was measured. However, under 0.5 or 1 mM Al treatment, after showing a slight decrease for 4 h, Fv/Fm began to show a sudden and rapid decline to low levels (0.500~0.600) over an 8-h period. On the other hand, Y (II) levels under growth illumination conditions also showed a time- and concentration-dependent decrease under Al treatment (**Fig. 3F**). After exposure to all three concentrations of Al,

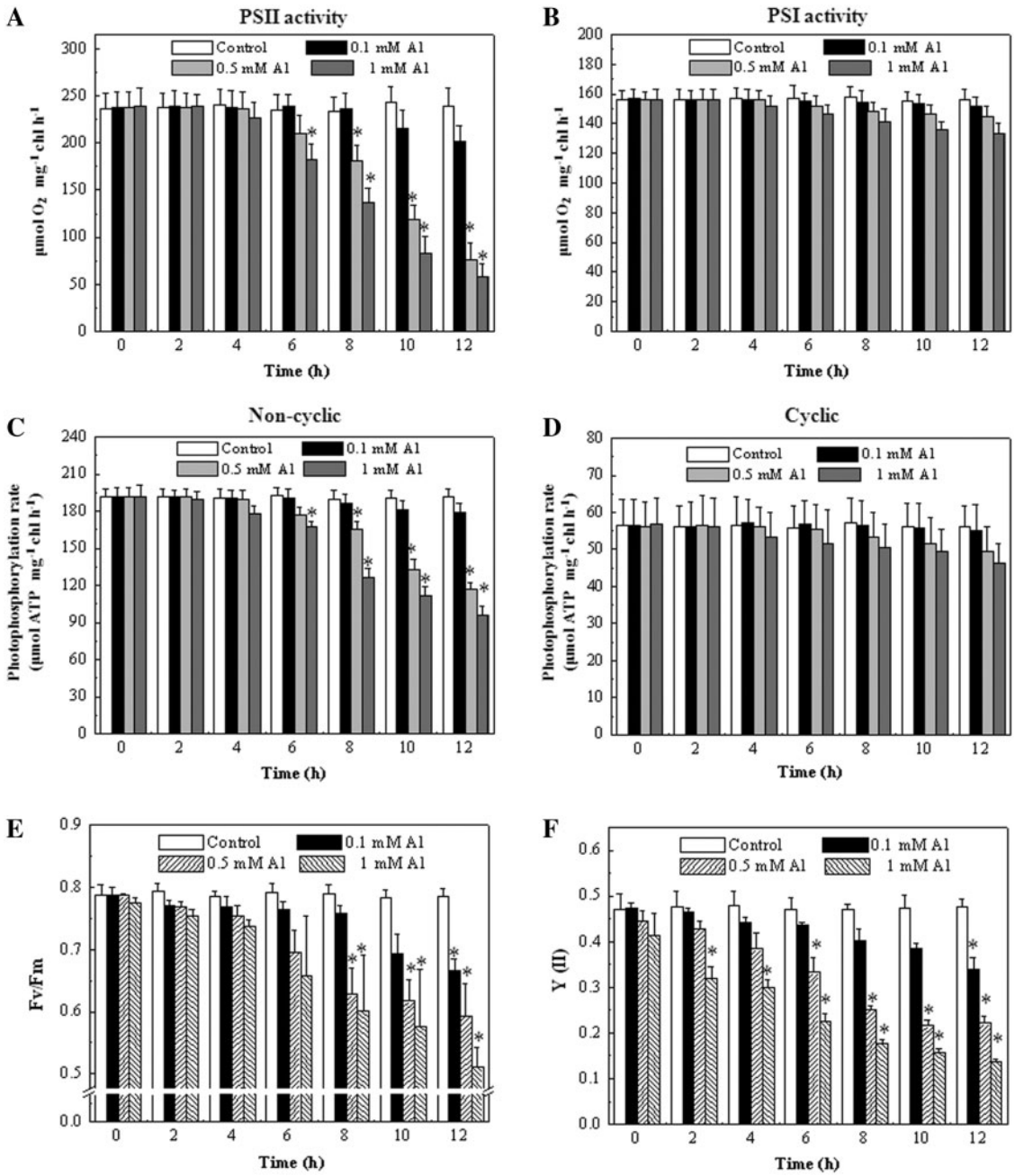

Fig. 3 Analysis of PSII and PSI activities under Al treatment. (A, B) Measurement of PSII and PSI electron transport activities using oxygen electrode. (C, D) Effect of Al treatment on the cyclic and non-cyclic photophosphorylation. (E) Quantitative analysis of time- and concentration-dependent changes of maximum PSII quantum yield Fv/Fm under Al treatment. (F) Quantitative analysis of time- and concentration-dependent effective PSII quantum yield Y (II) under Al treatment. Data are means ± SD of six independent experiments. Asterisks indicate a significant difference from the control at $P < 0.05$ by *t*-test.

values of Y (II) exhibited a time-dependent decrease from 2 to 12 h, but the magnitude and speed of the decline were greater with increased concentrations of Al treatment (**Fig. 3F**). The decrease of Y (II) appeared to precede the decline in Fv/Fm: often Y (II) fell to ≤50% of normal levels before the changes in Fv/Fm were noted, which is consistent with previous reports (Bonfig et al. 2006). Hence, the chlorophyll fluorescence experiments further demonstrated that PSII was the sensitive and major damage target of Al toxicity.

Al-induced PSII photochemical damage is ROS independent

ROS generation occurs in different cellular compartments and plays crucial roles in stress response (Apel and Hirt 2004).

Therefore, the double-staining technique was exploited to monitor intracellular ROS localization under a laser confocal scanning microscope (LCSM) at the single-cell level in vivo using 2′,7′-dichlorodihydrofluorescein diacetate (H_2DCFDA) staining. H_2DCFDA is a non-fluorescent compound that can readily enter cells. Once inside cells, the acetate is cleaved by endogenous esterases. The acetate-free, reduced form of H_2DCF is trapped inside the cells and can be oxidized by H_2O_2 to form DCF, a highly fluorescent compound (Li and Xing 2011). The data showed that bright DCF fluorescence was colocalized in cytoplasmic areas in which mitochondria were present, and could be detected at 10–20 min after treatment with 0.5 mM Al in the protoplasts double-stained with DCF and the mitochondria-specific probe MitoTracker Red CMXRos (**Fig. 4A**). At 30 min of treatment, the accumulated DCF fluorescence in the protoplasts largely occurred in the regions where chloroplasts were located and could be abolished by pretreatment with the ROS scavenger ascorbic acid (AsA) (**Fig. 4A**). Moreover, measurement of the DCF fluorescence intensity in isolated chloroplasts under 0.5 mM Al treatment indicated that chloroplasts were sources of Al-induced ROS production (**Fig. 4B**).

To establish whether the Al-induced photosynthetic damage was ROS dependent, the natural antioxidant AsA was used. As shown in **Fig. 5**, pre-incubation with AsA failed to alleviate the apparent decrease in DF and Fv/Fm values under Al stress ($P < 0.05$), while the decline in DF and Fv/Fm values were effectively inhibited by pretreatment with Lumogallion, which can chelate Al ions ($P > 0.05$; **Fig. 5A, B**). These results suggest that photosynthetic electron transfer chain components, especially PSII, might be directly damaged by Al instead of in an ROS-dependent manner.

Detection of Al accumulation in chloroplasts after Al treatment

In order to monitor whether Al accumulated in chloroplasts, the fluorescent probe Lumogallion, which emits green fluorescence after chelation with Al ions (Silva et al. 2000; Babourina and Rengel 2009), was used. The imaging results showed that with the extension of the treatment time the green fluorescence gradually increased (**Fig. 6A, B**). During 5–15 min after Al treatment, the fluorescence was colocalized in the cytoplasm and at 30 min the accumulated Lumogallion fluorescence in the protoplasts largely occurred in the regions where chloroplasts were located (**Fig. 6A**).

For further confirmation, the Al content in the chloroplast proteins isolated from 0.5 mM Al-treated leaves was determined by atomic absorption spectroscopy (AAS). The data showed that after 6 and 12 h of treatment, the Al content in the chloroplast proteins was obviously increased ($P < 0.05$); notably, the Fe content in the chloroplast proteins exhibited a gradual decline instead ($P < 0.05$; **Fig. 7**). These results indicate that Al ions entered and localized in the chloroplasts, and might interact with Fe ions in chloroplast proteins.

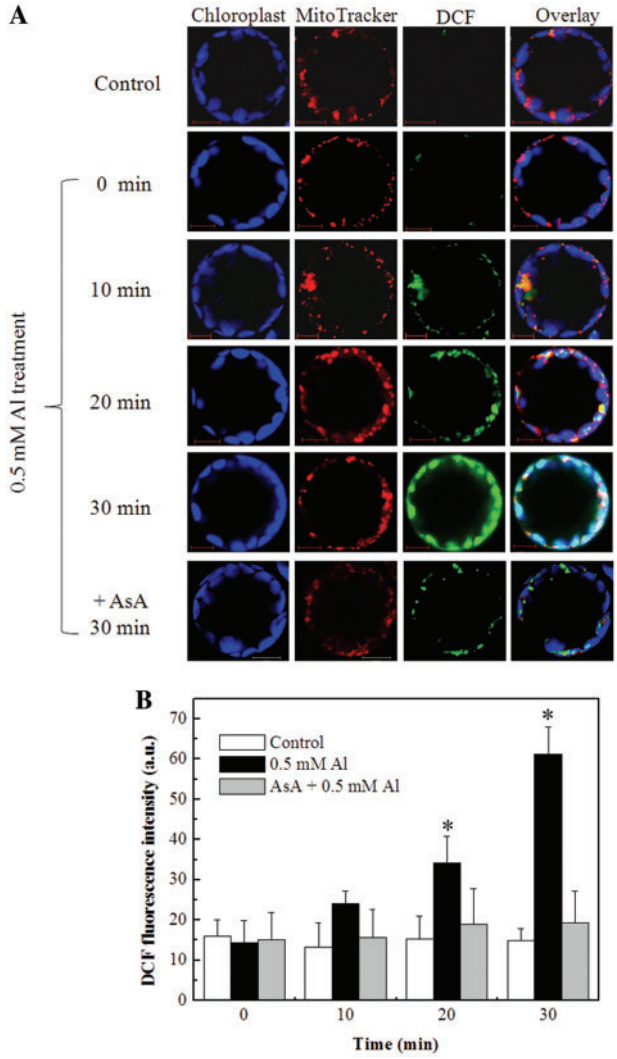

Fig. 4 Intracellular ROS production and localization in protoplasts after Al treatment. (A) Protoplasts were treated with Al for the indicated time period, double-stained with H_2DCFDA (at the final concentration of 5 μM) and MitoTracker Red CMXRos (at the final concentration of 100 nM), and observed by a laser scanning confocal microscope as described in Materials and Methods section. Scale bars = 10 μm. (B) Measurement of ROS production in isolated chloroplasts under Al treatment. Data are means ± SD of six independent experiments. Asterisks indicate a significant difference from the control at $P < 0.05$ by *t*-test. Before Al treatment, protoplasts or isolated chloroplasts were pretreated with AsA at the final concentration of 1 mM for 60 min.

Effects of Al treatment on the donor and acceptor sides of PSII

The above experiments demonstrated that PSII is the sensitive and major damage site of Al in the photosynthetic electron transfer chain; hence, we further characterized the inhibitory effect of Al on the donor and acceptor sides of electron transfer. PSII donor-side activity was evaluated by oxygen evolution in the presence of silicomolybdate, which acted as an artificial

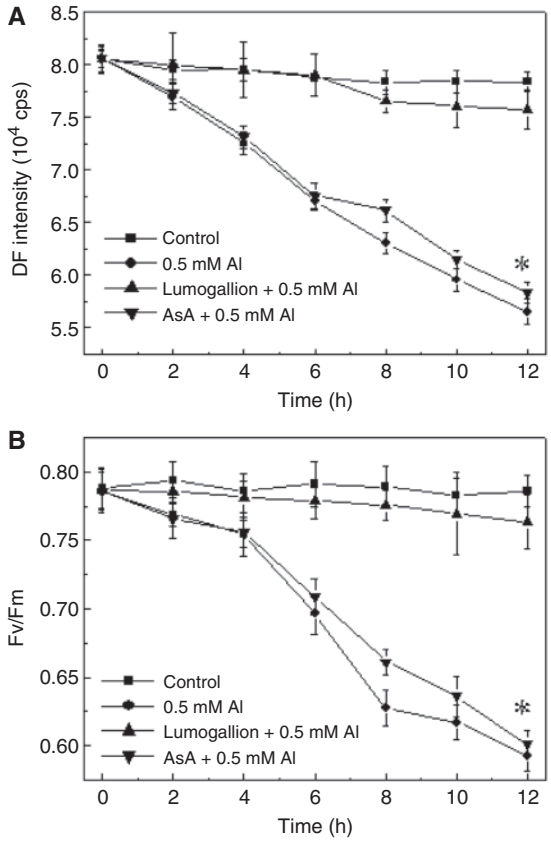

Fig. 5 Effect of Lumogallion and AsA on the damage to the photosynthetic rate and PSII activity. (A) Effects of Lumogallion and AsA on Al-induced decrease of DF. (B) Effects of Lumogallion and AsA on Al-induced decrease of Fv/Fm. Before 0.5 mM Al treatment, leaves were pretreated with AsA at the final concentration of 1 mM or Lumogallion at the final concentration of 100 μM for 60 min. Data are means ± SD of six independent experiments. Asterisks indicate a significant difference from the control at $P < 0.05$ by *t*-test.

electron acceptor. PSII acceptor-side activity was estimated by the rate of electron flow from DPC to DCIP. The results showed that 0.5 mM Al treatment exerted no obvious inhibition on the PSII donor side ($P > 0.05$; **Fig. 8A**), but obviously inhibited the activity of the PSII acceptor side ($P < 0.05$; **Fig. 8B**), which could be alleviated by pretreatment with the Al-chelating reagent Lumogallion, but could not be alleviated by addition of the ROS scavenger AsA (**Fig. 8B**). The data implied that the acceptor side was damaged more severely than the donor side under Al stress.

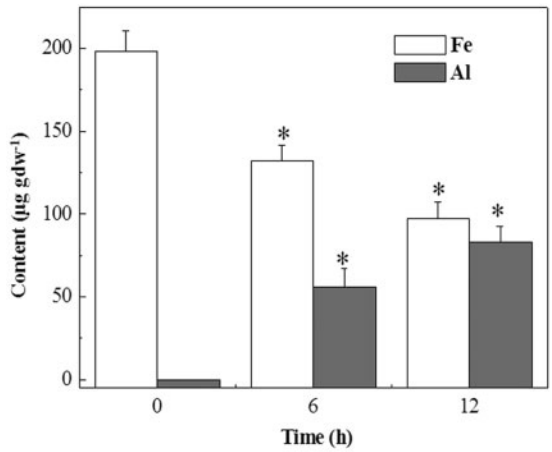

Fig. 7 Determination of Al and Fe contents in isolated chloroplast proteins by AAS. Chloroplast proteins were isolated after different time lengths of 0.5 mM Al treatment, and the contents of Al and Fe were determined by AAS as described in the Materials and Methods section. Data are means ± SD of three independent experiments. Asterisks indicate a significant difference from the control at $P < 0.05$ by *t*-test.

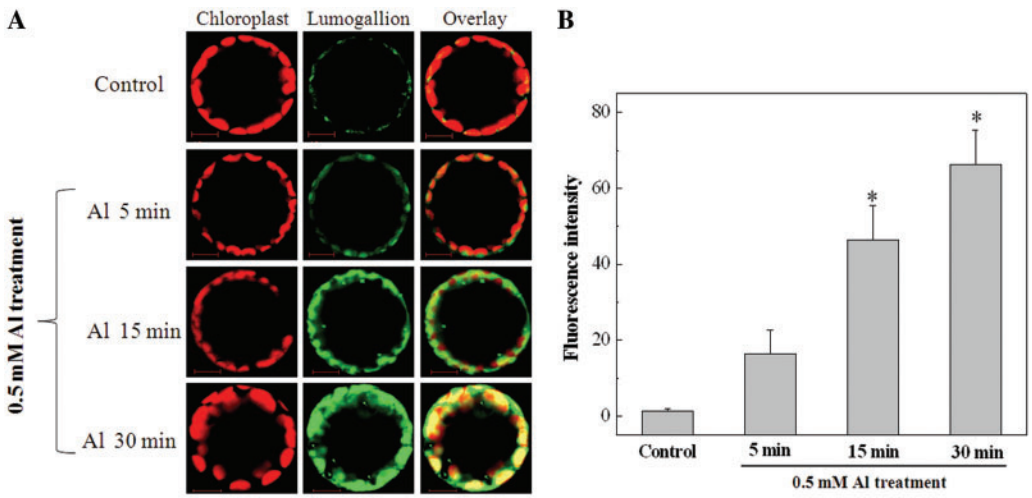

Fig. 6 Imaging and subcellular location of Al in Al-treated tobacco protoplasts. (A) The fluorescence imaging of Lumogallion and chloroplast autofluorescence in tobacco protoplasts after Al treatment. After 0.5 mM Al treatment, protoplasts were stained with Lumogallion at the final concentration of 100 μM for 60 min. Scale bars = 10 μm. (B) Intensity of Lumogallion fluorescence shown in (A). Data are means ± SD of three independent experiments. Asterisks indicate a significant difference from the control at $P < 0.05$ by *t*-test.

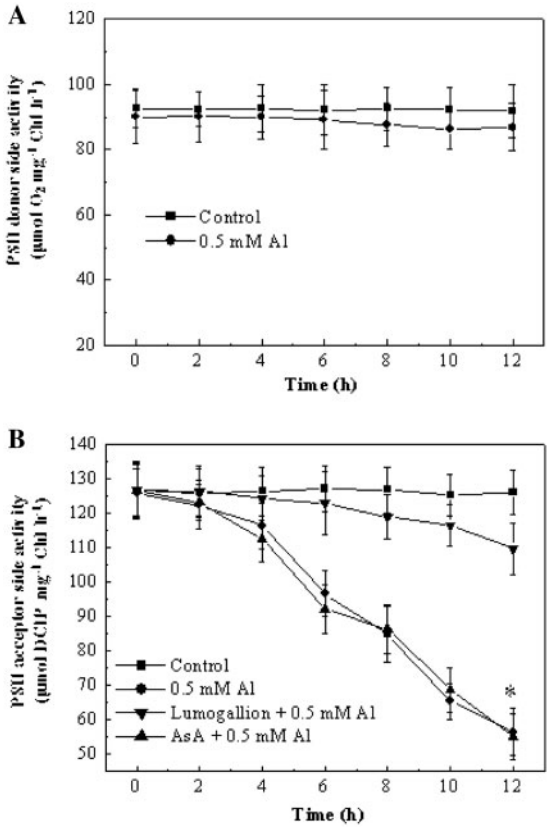

Fig. 8 Effect of Al on the donor side and acceptor side of PSII. (A) Effect of Al on the donor side of PSII. PSII donor-side activity was evaluated by oxygen evolution in the presence of silicomolybdate, which acted as an artificial electron acceptor. (B) Effect of Al on the acceptor side of PSII. PSII acceptor-side activity was estimated by the electron flow rate from DPC to DCIP. Before 0.5 mM Al treatment, leaves were pretreated with AsA at the final concentration of 1 mM or Lumogallion at the final concentration of 100 μM for 60 min. Data are means ± SD of three independent experiments. Asterisks indicate a significant difference from the control at $P < 0.05$ by *t*-test.

Al treatment inhibits electron transfer between Q_A and Q_B

To further investigate the inhibitory effect of Al on the accepter side of PSII electron transfer, we measured the state of Q_A and Q_B in Al-treated leaves. Flash-induced chlorophyll fluorescence decay kinetics is a portable, effective and non-invasive method to investigate the function of the PSII acceptor side (Huang et al. 2008; Wodala et al. 2008; Cai et al. 2010). Hence, the chlorophyll fluorescence decay curves were measured to reflect the Q_A^- reoxidation kinetics in Al-treated tobacco leaves. A short saturating light pulse reduced Q_A, causing a rapid increase in the fluorescence yield, followed by decay in the subsequent dark period due to Q_A^- reoxidation. The curves from untreated samples were characterized by a fast (approximately 176 μs), medium (approximately 2.6 ms) and slow (approximately 4.4 s) phase (**Fig. 9**; **Table 1**). In Al-treated leaves, the amplitude values of the fast (a_1) and middle (a_2) phases were both decreased. Treatment with 0.5 mM Al decreased the amplitude values of the fast phase (a_1) from 73% to 66% at 6 h and to 51% at 12 h. Similarly, the amplitude values of the middle phase (a_2) following 0.5 mM Al treatment were decreased from 21% to 14% at 6 h and to 12% at 12 h (**Table 1**). Instead, the amplitude values of the slow phase (a_3) were increased in Al-treated leaves. The amplitude values of the slow phase (a_3) following 0.5 mM Al treatment were increased from 6% to 20% at 6 h and to 37% at 12 h (**Table 1**). Furthermore, in the fast phase, 0.5 mM Al decreased the time constants (τ_1) to 135 and 96 μs at 6 and 12 h, respectively, and in the middle phase the time constants (τ_2) increased to 3.1 and 4.5 ms at 6 and 12 h, respectively (**Table 1**). These results suggested the Al-induced inhibition of electron transfer between Q_A and Q_B. Moreover, the inhibition could be alleviated by pretreatment with the Al-chelating reagent Lumogallion, but could not be alleviated by addition of the ROS scavenger AsA (**Fig. 9A, B**; **Table 1**).

In the DF decay curve, the fast phase (≤500 ms) is proportional to the Q_A^- amount and the slow phase (>500 ms) is proportional to the Q_B^- amount. The inhibition of electron transfer between Q_A and Q_B, on the one hand, can cause the accumulation of e^- at the site of Q_A and increase the Q_A^- amount, to enhance the fast phase and decay the DF intensity more rapidly; on the other hand, it can cause the amount of Q_B^- to decrease, resulting in the lower level of the slow phase (Li et al. 2007). Our results showed that at 6 and 12 h of Al treatment, the fast phase of the DF decay curve was enhanced and the slow phase was lower (**Fig. 10A**), indicating the inhibition of electron transfer between Q_A and Q_B. Moreover, the inhibition could be alleviated by pretreatment with the Al-chelating reagent Lumogallion (**Fig. 10B**), but could not be alleviated by addition of the ROS scavenger AsA (**Fig. 10C**).

For further confirmation, the effect of Al treatment on specific chlorophyll fluorescence parameters that can reflect the state of Q_A and Q_B was investigated. The steady-state qP and the variable fluorescence Fv can reflect the state of Q_A: lower values of qP are proportional to higher amounts of Q_A^- (Wodala et al. 2008) and higher values of Fv are proportional to higher amounts of Q_A^- (Zhang et al. 2003), both indicating the inhibition of electron transfer between Q_A and Q_B. The data exhibited that qP values underwent a time- and concentration-dependent decrease (**Figs. 11A, S1B**), while the Fv values went through a time- and concentration-dependent increase (**Figs. 11B, S1C**). Also, their changes could be alleviated by pretreatment with the Al-chelating reagent Lumogallion, but could not be alleviated by addition of the ROS scavenger AsA (**Fig. 11C, D**). These results were in good correlation with the measurement of chlorophyll fluorescence decay kinetics and DF decay kinetics, implicating the accumulation of the reduced form of the electron accepter Q_A^-. Notably, pretreatment experiments suggested that the accumulation of Q_A^- might be directly caused by Al instead of in an ROS-dependent manner.

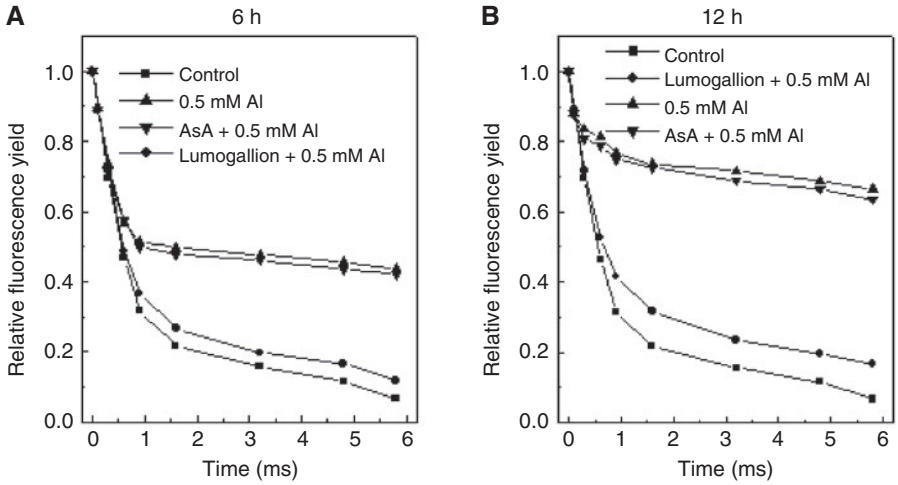

Fig. 9 Effect of Al on chlorophyll fluorescence decay kinetics. Measurements were carried out on leaves with or without Lumogallion or AsA pretreatment at 6 h (A) and 12 h (B) under Al stress. Before 0.5 mM Al treatment, leaves were pretreated with AsA at the final concentration of 1 mM or Lumogallion at the final concentration of 100 μM for 60 min. Curves were normalized to the same amplitude and each trace is the average of five measurements.

Table 1 Decay kinetics parameters of flash-induced variable fluorescence in tobacco leaves under Al treatment

Treatment	Fast phase τ_1 (a_1)	Middle phase τ_2 (a_2)	Slow phase τ_3 (a_3)
Control	176 ± 12 μs (73%)	2.6 ± 1.1 ms (21%)	4.4 ± 1.3 s (6%)
0.5 mM Al, 6 h	135 ± 9 μs (66%)	3.1 ± 0.9 ms (14%)	3.3 ± 1.1 s (20%)
0.5 mM Al, 12 h	96 ± 11 μs (51%)	4.5 ± 1.2 ms (12%)	2.8 ± 0.8 s (37%)
Pre-treatment with Lumogallion			
0.5 mM Al, 6 h	171 ± 10 μs (74%)	2.8 ± 0.6 ms (22%)	4.3 ± 1.1 s (4%)
0.5 mM Al, 12 h	168 ± 9 μs (72%)	2.9 ± 0.5 ms (23%)	3.6 ± 0.6 s (5%)
Pre-treatment with AsA			
0.5 mM Al, 6 h	132 ± 8 μs (63%)	2.8 ± 0.9 ms (15%)	3.4 ± 1.2 s (22%)
0.5 mM Al, 12 h	98 ± 13 μs (51%)	4.1 ± 1.3 ms (15%)	3.1 ± 1.0 s (34%)

Measurements were performed on leaf discs, as in **Fig. 9**, that were incubated for 6 or 12 h under 120 μmol quanta m^{-2} s^{-1} white light in distilled water (control) or solutions containing 0.5 mM Al, and then dark adapted for 15 min. Exponential analyses yielded triphasic kinetics with different half-life (τ) and amplitudes (a). Mean values ± SD were calculated from five measurements.

Effects of Al treatment on steady-state NPQ

The rate of the light-dependent acidification of the lumen depends on the rate of electron transport and also on the activity of ATP synthase (Wodala et al. 2008). The Al-derived inhibition of the linear electron transport of PSII should reduce proton accumulation in the lumen, which would then cause a decrease in NPQ via the energy-dependent quenching (qE) component. Al treatment decreased the steady-state NPQ, as well as qE and photoinhibitory quenching components in a concentration-dependent manner, and this effect was eliminated by pretreatment with Lumogallion instead of AsA (**Fig. S2**).

Discussion

Our current work investigated the mechanism of how PSII photochemical activity was affected by Al and characterized the target site of Al in photosynthetic electron transport, providing new insight into the mechanism of Al phytotoxicity-induced chloroplast dysfunction and photosynthetic damage.

Al toxicity is a major factor limiting crop productivity in acid soils, through causing photosynthetic damage including pigment degradation, carbon assimilation inhibition and decreased photosynthetic electron transport (Akaya and Takenaka 2001; Chen et al. 2005; Mihailovic et al. 2008). Our present results showed that values of both DF and Pn exhibited a time- and concentration-dependent decrease (**Fig. 1**), and the electron transport capacity was inhibited by Al treatment as well (**Fig. 2**), indicating the photosynthetic damage induced by Al. In the photosynthetic electron transport chain, PSII is a complex that catalyses electron transfer from water to plastoquinone, a diffusible molecule that connects PSII to the next component in the chain. It is well known that PSII is most

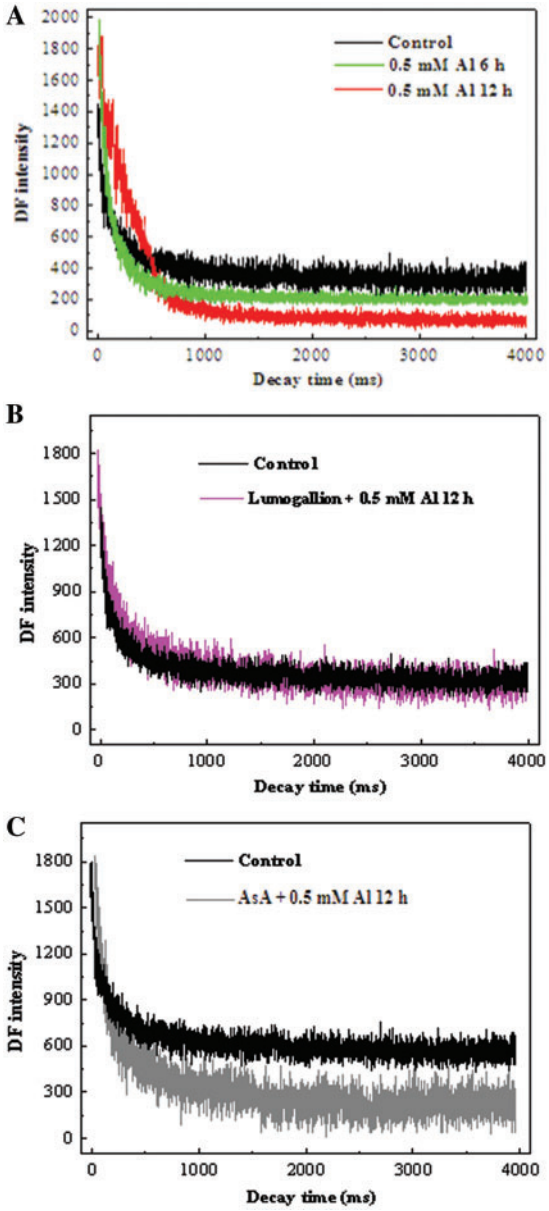

Fig. 10 Changes of the DF decay curve of tobacco leaves after Al treatment. (A) Time-dependent change of the DF decay curve under 0.5 mM Al treatment. (B) Effect of Lumogallion on the Al-induced change of the DF decay curve. (C) Effect of AsA on the Al-induced change of the DF decay curve. Before 0.5 mM Al treatment, leaves were pretreated with AsA at the final concentration of 1 mM or Lumogallion at the final concentration of 100 μM for 60 min. The DF decay curve was obtained according to the Materials and Methods section. Results are from a single analysis, representative of three independent experiments that yielded similar results.

sensitive to environmental stresses and it is considered to play key roles in the response of photosynthesis to environmental perturbations, including Al phytotoxicity (Lu et al. 2003; Chen et al. 2005; Farage et al. 2006; Ehlert and Hincha 2008; Jiang et al. 2008; Zhao et al. 2008). Our results measuring PS activities and photophosphorylation rates showed that Al treatment caused much more severe damage to PSII than to PSI (**Fig. 3A–D**), suggesting that PSII was the sensitive and major target of Al toxicity. As the photosynthetic machinery is demonstrated to be regulated at the levels of the reaction center, energy absorption, energy dissipation, excitation energy trapping and electron transport under adverse environments (Samuilov et al. 2003; Tanaka and Tanaka 2006), our investigation of the maximum (Fv/Fm) and operating (Y (II)) efficiencies of PSII demonstrated the damage to the PSII photochemical capacity induced by Al (**Fig. 3E, F**; **Fig. S1A**). As no 'light pressure' was applied, a decrease of Fv/Fm cannot reflect any downstream limitation in the photosynthetic electron transport, e.g. in the Calvin–Benson cycle. Therefore, it must reflect inhibition in the direct vicinity of the PSII reaction centers or be due to secondary damage caused by photoinhibition, which is known to affect PSII centers (Bonfig et al. 2006; Berger et al. 2007). As described in previous work by Kramer et al. (2004), the Imaging-PAM Chlorophyll Fluorometer allows the assessment of Y (II), Y (NPQ) and Y (NO), which add up to unity. While both Y (NO) and Y (NPQ) reflect fractions of excitation energy being lost as heat, high Y (NO) values in contrast to high Y (NPQ) values are indicative of irreversible damage (Kanazawa and Kramer 2002; Kramer et al. 2004). The data of **Fig. S3** clearly illustrate that Y (NO) increased at the cost of Y (II) and Y (NPQ) as Al stress progressed (**Fig. S3**), indicating irreversible damage to PSII. Our results further demonstrated that the acceptor side of PSII was damaged more severely than the donor side under Al stress (**Fig. 8**). This work characterized a concentration- and time-dependent decrease of PSII activity, especially the acceptor side under Al stress, validating and further advancing previous knowledge of Al-induced photosynthetic damage (Jiang et al. 2008).

In the study of adverse stresses, ROS have been recognized as playing crucial roles both in animal and plant cells (Simon et al. 2000; Van Breusegem and Dat 2006). As the specific organelle that is responsible for energy capture in plants, chloroplasts, on the one hand, are the prime site of ROS production; on the other hand, they are the sensitive targets of ROS attack, and may generate intermediate signals involved in plant stress responses and programmed cell death (Vitaly et al. 2003; Baier and Dietz 2005; Tanaka and Tanaka 2006). In our experiments, a quick burst of ROS formation occurred in Al-treated protoplasts and the ROS generated from chloroplasts were demonstrated to be involved in the oxidative burst induced by Al (**Fig. 4**). However, the pretreatment experiments with AsA and Lumogallion indicated that the decrease in the photosynthetic capacity and the damage to PSII might be directly caused by Al instead of in an ROS-dependent manner (**Figs. 5**, **8**). Furthermore, we found that after entering the cells, Al accumulated in the chloroplasts, resulting in the decreased Fe content of chloroplast proteins (**Figs. 6**, **7**), leading us to investigate the mechanism of how Al ion affects chloroplast function.

Al and Fe ions have highly similar chemical characteristics, and in some cases Al can replace Fe in Fe-containing proteins and Fe transporters (Fleming and Joshi 1987; Cannata-Andia

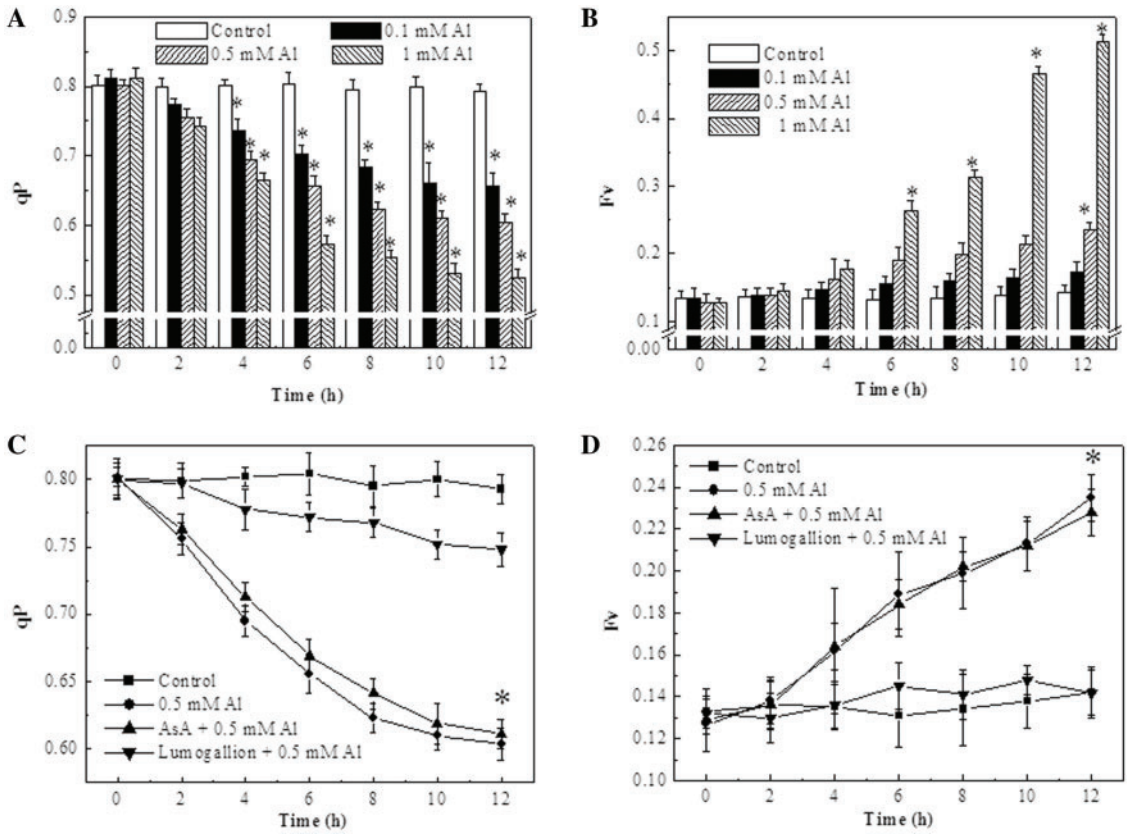

Fig. 11 Changes of the chlorophyll fluorescence parameter qP and Fv under Al treatment. (A, B) Quantitative analysis of the time- and concentration-dependent changes of qP and Fv under Al treatment. (C, D) Effects of Lumogallion and AsA on the changes of qP and Fv induced by Al. After pretreatment with Lumogallion (100 μM) or AsA (1 mM), respectively, for 60 min, leaves were treated with 0.5 mM Al, and the chlorophyll fluorescence parameters qP (C) and Fv (D) were measured at the indicated times. Data are means ± SD of six independent experiments. Asterisks indicate a significant difference from the control at $P < 0.05$ by *t*-test.

1996). As previously described, Al, through replacing one of the Fe ions or being present in addition to the Fe ions, can directly interact with Fe-S proteins to cause the decreased activities of complex I and III in the mitochondrial electron transport chain, resulting in the subsequent mitochondrial oxidative burst (Panda et al. 2008; Li and Xing 2011). On the acceptor side of PSII electron transport, non-heme iron is present in the linear $Q_AFe^{2+}Q_B$ complex. The non-heme iron (II) forms coordinate covalent bonds with four His residues provided by the D1 and D2 reaction center subunits, and control the rate of electron transfer between Q_A and Q_B (Petrouleas and Diner 1990; Kern et al. 2005; Wodala et al. 2008). Our DF fluorescence and chlorophyll fluorescence experiments showed a decreased rate of electron transport between Q_A and Q_B upon Al treatment, which could not be alleviated by eliminating ROS (**Figs. 9–11**, **Table 1**). These results provide strong in vivo evidence in support of the competitive interaction or replacement of non-heme iron with Al, causing inhibition of the electron transport between Q_A and Q_B (**Fig. 12B**). The rate of light-dependent acidification of the lumen depends on the rate of electron transport and also on the activity of ATP synthase (Wodala et al. 2008). Our results show that the Al-derived inhibition of linear electron transport of PSII reduced the proton accumulation in the lumen and caused a decrease in the steady-state NPQ via the qE component, providing circumstantial evidence for the inhibition of electron transport between Q_A and Q_B induced by Al stress (**Fig. S2**).

In conclusion, according to our experimental results, a potential cascade of events during Al-induced photosynthetic damage is proposed (**Fig. 12**): Al, after entering cells, accumulates in the chloroplasts, reacts with or replaces the non-heme iron between the Q_A and Q_B binding sites, and blocks PSII electron transport, resulting in PSII photochemical damage and the inhibition of photosynthesis. Our work detected the inhibition of the photosynthetic rate and the damage to PSII activity, characterized the target site of Al phytotoxicity in the photosynthetic electron transport chain, providing new insight into the mechanism of Al phytotoxicity-induced chloroplast dysfunction and photosynthetic damage.

Materials and Methods

Plant material and chemical reagents

Tobacco seedlings (*Nicotiana tabacum* L. cv.) used for all experiments were grown in soil culture in a growth chamber

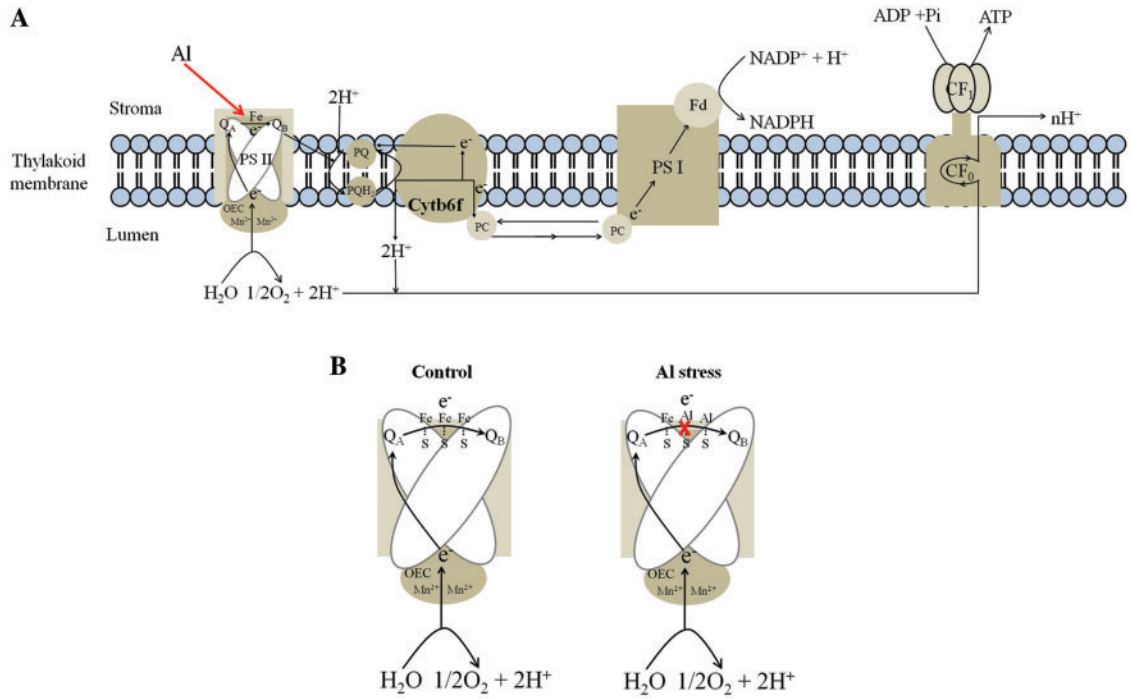

Fig. 12 Proposed working model for the inhibition of photosynthetic electron transport by Al (A) and the target site of Al on PSII (B).

(model E7/2; Conviron, Winnipeg, Canada) with a 16-h light photoperiod (120 μmol quanta m^{-2} s^{-1}) and a relative humidity of 75/80% at 23/21°C (light/dark) for 4 weeks.

H_2DCFDA and MitoTracker Red CMXRos were obtained from Molecular Probes (Eugene, OR, USA). Lumogallion was obtained from TCI (Shanghai, China). AsA was purchased from Sigma–Aldrich (Shanghai, China).

Al application

To treat tobacco leaves, entire leaves detached from 4-week-old seedlings were immersed in MS solution (pH 4.5) in the presence or absence of different concentrations of Al with or without the pretreatment of AsA or Lumogallion. To treat tobacco protoplasts, $AlCl_3$ solutions (pH 4.5) at the indicated concentrations were added to 100 μl of protoplast suspension in 96-well plates and incubated for the required time at room temperature.

Treatment with AsA and Lumogallion

Before Al treatment, the tobacco leaves were pre-incubated with AsA or Lumogallion for 60 min in MS solution. AsA was used at a final concentration of 1 mM and Lumogallion was used at a final concentration of 100 μM.

Pn measurement

The Pn of the leaves of 4-week-old tobacco seedlings was measured using a commercially available system (LI-6400; LI-COR, Inc., Lincoln, NE, USA) equipped with a 6400-15 Chamber (1.0 cm in diameter) and artificial illumination (irradiated by a modulated tungsten lamp) (Zhang and Xing 2008). The Pn of the leaves treated with Al was determined in a leaf chamber with a CO_2 concentration of 400 ppm after the leaves in the leaf cuvette were irradiated with a saturated irradiation of 1000 μmol quanta m^{-2} s^{-1} for about 15 min. The relative humidity and temperature of the leaf cuvette were about 85% and 22°C, respectively.

Photochemical efficiency measurement

The photochemical efficiency of the leaves detached from 4-week-old tobacco seedlings was quantified by measuring chlorophyll DF. The DF of chloroplasts, which is mainly emitted from PSII through inverse photochemical reactions, is an intrinsic label of the efficiency of charge separation at P680. The DF of intact leaves from tobacco seedlings was recorded with a custom-built DF detection system. The technical details of the system are described in our previous studies (Wang et al. 2007; Zhang and Xing 2008). Here, a brief summary of the measurement process is presented. After Pn measurement, the leaves were placed inside the system's chambers to dark-adapt for 5 min before the irradiation source was turned on. After a 0.2 s illumination period (400 μmol quanta m^{-2} s^{-1}) and a 0.26 s delay period, DF from the samples was collected by an independent optical fiber bundle and transmitted to corresponding ultra-high-sensitive single-photon counting modules [SPCMs (MP963, Perkin-Elmer, Wiesbaden, Germany)] with a wavelength detection range of 185–850 nm. The output signals, which had been amplified and discriminated by the

SPCMs, were further processed by a digital signal processor (TMS320C6416) or a computer to obtain the DF decay curve. The DF intensity, which was integrated from 0.26 to 5.26 s under the DF decay curve, was presented as counts per second (cps). The DF intensity was obtained by integration between 0.26 and 5.26 s in the DF decay dynamics curve. The data collection started at 0.26 s upon completion of the light irradiation and lasted for 5 s, because the DF signal was stable at 0.26 s and decreased to nearly zero at 5.26 s. The DF intensity of seven independent replicates was simultaneously measured by opening seven channels of the multichannel biosensor. All measurements were performed in the dark at 25°C.

Imaging and measurement of chlorophyll fluorescence parameters

A portable version of an Imaging-PAM Chlorophyll Fluorometer (PAM-MINI, Walz, Effeltrich, Germany) connected to a computer with data acquisition software (ImagingWin v2.0 m, Walz) was used. The experimental procedures followed those reported previously (Schreiber 2004; Bonfig et al. 2006; Wodala et al. 2008). After Al treatment, leaves were dark adapted for ≥15 min for precise determination of the minimal and maximal fluorescence levels in the dark (Fo and Fm, respectively). Fm was obtained by exposing the leaf sample to a high intensity (8,000 μmol quanta m^{-2} s^{-1}) short pulse (0.8 s). The maximum PSII quantum yield (Fv/Fm) was automatically calculated by the ImagingWin software (Walz). Maximum fluorescence values in the light-adapted state (Fm′) were determined at the end of a 30-min actinic light illumination with 130 μmol quanta m^{-2} s^{-1}. After switching the actinic light off, far-red light was applied to determine the minimal level of fluorescence at steady state (Fo′). The effective PSII quantum yield [Y (II)] was automatically derived by the ImagingWin software (Walz). At a known flux of incident PAR, the ETR was calculated. The effective PSII quantum yields of regulated non-photochemical energy dissipation, Y (NPQ), and non-regulated energy dissipation, Y (NO), which were complementary with the photochemical quantum yield [Y (II) + Y (NPQ) + Y (NO) = 1] were calculated by the ImagingWin software. Steady-state qP [(Fm′ − Fs)/Fm′ − Fo′] was automatically calculated by the ImagingWin software (Walz). Fs was the steady-state fluorescence yield during actinic illumination. Steady-state NPQ was calculated as: NPQ = (Fm − Fm′)/Fm′. The relaxation kinetics of steady-state NPQ was monitored by applying saturating pulses with 60-s intervals from the end of the 30-min actinic illumination period to determine the qE component of NPQ. qE relaxed in the first 5 min of the dark relaxation period and was calculated as: qE = Fm/Fm′ − Fm/Fm″, where Fm″ is the maximum fluorescence yield in the fifth min of dark relaxation subsequent to the illumination period. Images of the fluorescence parameters were displayed with the help of a false color code, ranging from 0.000 (black) to 1.000 (purple).

Measurement of chlorophyll fluorescence decay kinetics

The decay of chlorophyll a fluorescence yield after a single-turnover flash was measured with a double-modulation fluorescence fluorometer (model FL-200, Photon Systems Instruments, Brno, Czech Republic) (Trtilek et al. 1997; Cai et al. 2010). The instrument contained red LEDs for both actinic (20 μs) and measuring (2.5 μs) flashes, and was used in the time range of 100 μs to 100 s. With this type of measurement, it is important to avoid distortion of the relaxation kinetics due to the actinic effect of measuring flashes. This was carefully checked and the intensity of the measuring flashes was set at a value low enough to avoid a reduction of Q_A in the presence of DCMU.

Measurement of PSI and PSII activities

The photosynthetic electron transport activities were determined as described previously (Yang et al. 2008; Cai et al. 2010). At the indicated time after Al treatment, the fully expanded leaves were harvested and homogenized in a medium containing 0.4 M sucrose and 50 mM Tricine (pH 7.6). The homogenate was filtrated through 16 layers of gauze and the filtrate was then centrifuged at 500 × g for 3 min to remove large debris. The supernatant was further centrifuged at 3,000 × g for 10 min. The pellet was washed twice with buffer (50 mM Tricine, 10 mM NaCl, 5 mM $MgCl_2$, pH 7.6) at 10,000 × g for 10 min. The resulting washed pellet of thylakoid membranes was resuspended in the same buffer for measuring the electron transport activities. The electron transport activities in the thylakoid membranes were measured with a Clark-type oxygen electrode (Hansatech, King's Lynn, Norfolk, UK) suspended in the medium (0.4 M sucrose, 50 mM Tricine, 10 mM NaCl, 5 mM $MgCl_2$, pH 7.6) under growth light intensity (120 μmol quanta m^{-2} s^{-1}). PSI electron transport activity was measured with 10 mM methylamine, 10 μM DCMU, 1 mM sodium azide, 500 μM DCIP, 2 mM sodium ascorbate and 1 mM methyl viologen. PSII electron transport activity was determined using 1 mM phenyl-*p*-benzoquinone as the electron acceptor.

Assay of cyclic and non-cyclic photophosphorylation rates

The photophosphorylation activity of chloroplasts was assayed by using the luciferin–luciferase method to measure the amount of ATP synthesized within 2 min at a saturating irradiance of about 1,500 μmol quanta m^{-2} s^{-1} and 25°C, as previously described (Huang et al. 2008). Cyclic photophosphorylation activity was determined in 1 cm^3 of reaction mixture containing 50 mM Tricine-KOH (pH 8.0), 2 mM $MgCl_2$, 1 mM ADP, 5 mM phosphate (Pi), 0.05 mM phenazine methosulfate (PMS) and chloroplasts containing about 10 μg of chlorophyll. Non-cyclic photophosphorylation activity was assayed similarly to cyclic photophosphorylation, except that

PMS was replaced by 1 mM FeCy. The reactions were stopped by placing the test tubes into boiling water for 3 min.

Measurement of the acceptor-side and donor-side activities of PSII

The activity of the PSII acceptor side was assayed according to the method of Huang et al. 2008. The rate of PSII photoreduction of DCIP with the addition of the artificial electron donor DPC was measured photometrically (ΔA580, 12.9 mM^{-1} cm^{-1}) at 25°C in a medium containing 130 mM NaCl, 30 μM DCIP, 50 mM $CaCl_2$ and 50 mM MES-NaOH (pH 6.0). The concentration of DPC was 150 μM and the concentration of chloroplasts isolated from tobacco leaves was equivalent to 10 μg chlorophyll ml^{-1}. Actinic light was provided by an incandescent lamp combined with a heat-absorbing filter and a red cut-off filter.

The activity of the PSII donor side was measured in assay buffer [5 mM $MgCl_2$, 10 mM NaCl, 330 mM sorbitol, 20 mM Tricine (pH 7.6), 2 mM $CaCl_2$, 5 mM NH_4Cl] with silicomolybdate, which acted as an artificial electron acceptor, using a Clark-type oxygen electrode (Hansatech, King's Lynn, Norfolk, UK) at 25°C (Kim et al. 2007). The concentration of silicomolybdate was 0.19 mM and the concentration of chloroplasts isolated from tobacco leaves was equivalent to 10 μg chlorophyll ml^{-1}.

Fluorescence imaging of confocal microscopy

All microscopic observations were performed using a Zeiss LCSM (LSM510/ConfoCor2, Carl-Zeiss, Jena, Germany). The H_2DCFDA (at the final concentration of 5 μM) and Lumogallion (at the final concentration of 100 μM) signals were visualized with excitation at 488 nm and emission at 500—550 nm using a band-pass filter. Chloroplast autofluorescence (488-nm excitation) was visualized at 650 nm with a long-pass filter. The MitoTracker Red CMXRos (at the final concentration of 100 nM) signal was visualized in another detection channel using 543-nm excitation from a He-Ne laser and a 565–615-nm band-pass filter.

Isolation of tobacco mesophyll protoplasts

Small leaf strips (0.5–1 mm) in the enzyme solution including cellulase R10 and macerozyme R10 (Yakult Honsha, Tokyo, Japan) were vacuum infiltrated for about 30 min and then incubated in dark for 3 h. After filtration through a 75 -μm nylon mesh, the crude protoplast filtrates were sedimented by centrifugation for 3 min at 100 *g*. The purified protoplasts were suspended in W5 solution (154 mM NaCl, 125 mM $CaCl_2$, 5 mM KCl, 5 mM glucose, 1.5 mM MES-KOH, pH 5.6) and counted in a hematocytometer.

Isolation of chloroplasts from tobacco leaves

The isolated protoplasts were suspended in 2 ml of 0.05 M Tricine-NaOH buffer (pH 7.5) containing 0.5 M sucrose and 0.1% BSA, and then were ruptured through a syringe (0.5 × 4 cm, Termo). The ruptured protoplast preparations (0.5 ml) were directly layered on top of 15 ml of the linear sucrose gradient (35–60%, w/w) dissolved in 0.02 M Tricine-NaOH buffer (pH 7.5) and run at 24,000 rpm for 3 h at 4°C using a Beckman-Spinco SW 25-3 rotor. At the end of the run, 0.5-ml fractions were collected.

Measurement of ROS production in isolated chloroplasts

After incubation with 5 μM H_2DCFDA for 30 min, isolated chloroplasts (0.5 mg ml^{-1}) were treated with Al and the DCF fluorescence intensity was measured with an LS55 Luminescence Spectrophotometer (PerkinElmer, UK) at room temperature. The values at 525 nm were used to determine the fluorescence intensity of DCF.

Determination of metal ion content by AAS

The samples of chloroplasts isolated from Al-treated leaves were digested with acids, and the concentrations of Al and Fe were determined using an atomic absorption spectrophotometer with a graphite furnace atomizer (model Z-9000; Hitachi, Tokyo).

Statistical analysis

All assays were repeated independently for a minimum of three times. Data are presented as the mean ± SD. Statistical analysis was performed using the Student's paired *t*-test. Differences were considered statistically significant at $P < 0.05$.

Supplementary data

Supplementary data are available at PCP online.

Funding

This work was supported by the Program for Changjiang Scholars and Innovative Research Team in University (IRT0829), the Key Program of NSFC-Guangdong Joint Funds of China (U0931005), and the National High Technology Research and Development Program of China (863 Program) (2007AA10Z204).

Acknowledgments

We are grateful to Yonghong Tang, Lizhang Zeng and Jun Zhou for their excellent technical assistance and constructive discussions.

References

Akaya, M. and Takenaka, C. (2001) Effects of aluminum stress on photosynthesis of *Quercus glauca* Thumb. *Plant Soil* 237: 137–146.

Apel, K. and Hirt, H. (2004) Reactive oxygen species: metabolism, oxidative stress, and signal transduction. *Ann. Rev. Plant Biol.* 55: 373–399.

Appenroth, K.J., Stockel, J., Srivastava, A. and Strasser, R.J. (2001) Multiple effects of chromate on the photosynthetic apparatus of *Spirodela polyrhiza* as probed by OJIP chlorophyll a fluorescence measurements. *Environ. Pollut.* 115: 49–64.

Babourina, O. and Rengel, Z. (2009) Uptake of aluminum into Arabidopsis root cells measured by fluorescent lifetime imaging. *Ann. Bot. (Ldn.)* 104: 189–195.

Baier, M. and Dietz, K.J. (2005) Chloroplasts as source and target of cellular redox regulation: a discussion on chloroplast redox signals in the context of plant physiology. *J. Exp. Bot.* 416: 1449–1462.

Baker, N.R. and Rosenqvist, E. (2004) Applications of chlorophyll fluorescence can improve crop production strategies: an examination of future possibilities. *J. Exp. Bot.* 55: 1607–1621.

Berger, S., Benediktyova, Z., Matous, K., Bonfig, K., Mueller, M.J., Nedbal, L. et al. (2007) Visualization of dynamics of plant–pathogen interaction by novel combination of chlorophyll fluorescence imaging and statistical analysis: differential effects of virulent and avirulent strains of *P. syringae* and of oxylipins on *A. thaliana*. *J. Exp. Bot.* 58: 797–806.

Bonfig, K.B., Schreiber, U., Gabler, A., Roitsch, T. and Berger, S. (2006) Infection with virulent and avirulent *P. syringae* strains differentially affects photosynthesis and sink metabolism in *Arabidopsis* leaves. *Planta* 225: 1–12.

Cai, B., Zhang, A.H., Yang, Z.P., Lu, Q.T., Wen, X.G. and Lu, C.M. (2010) Characterization of photosystem II photochemistry in transgenic tobacco plants with lowered Rubisco activase content. *J. Plant Physiol.* 167: 1457–1465.

Cannata-Andia, J.B. (1996) Aluminum toxicity: its relationship with bone and iron metabolism. *Nephrol. Dial. Transpl.* 11: 69–73.

Chaerle, L. and Van Der Straeten, D. (2000) Imaging techniques and the early detection of plant stress. *Trends Plant Sci.* 5: 495–500.

Chen, L.S., Qi, Y.P. and Liu, X.H. (2005) Effects of aluminum on light energy utilization and photoprotective systems in citrus leaves. *Ann. Bot.* 96: 35–41.

Diner, B.A. and Petrouleas, V. (1990) Formation by NO of nitrosyl adducts of redox components of the photosystem II reaction center. II: Evidence that HCO_3^-/CO_2 binds to the acceptor-side non-heme iron. *Biochim. Biophys. Acta* 1015: 141–149.

Ehlert, B. and Hincha, D.K. (2008) Chlorophyll fluorescence imaging accurately quantifies freezing damage and cold acclimation responses in Arabidopsis leaves. *Plant Methods* 4: 12.

Farage, P.K., Blowers, D.A., Long, S.P. and Baker, N.R. (2006) Low growth temperatures modify the efficiency of light use by photosystem II for CO_2 assimilation in leaves of two chilling-sensitive C4 species, *Cyperus longus* and *Miscanthus* × *giganteus*. *Plant Cell Environ.* 29: 720–728.

Fleming, J. and Joshi, J.G. (1987) Ferritin: isolation of aluminum–ferritin complex from brain. *Proc. Natl. Acad. Sci. USA* 84: 7866–7870.

Giardi, M.T., Masojidek, J. and Godde, D. (1997) Effects of abiotic stresses on the turnover of the D1 reaction center II protein. *Physiol. Plant* 101: 635–642.

Goussias, C., Deligiannakis, Y., Sanakis, Y., Ioannidis, N. and Petrouleas, V. (2002) Probing subtle coordination changes in the iron–quinone complex of photosystem II during charge separation, by the use of NO. *Biochemistry* 41: 15212–15223.

Huang, H., Liu, X.Q., Qu, C.X., Liu, C., Chen, L. and Hong, F.H. (2008) Influences of calcium deficiency and cerium on the conversion efficiency of light energy of spinach. *Biometals* 21: 553–561.

Jiang, H.X., Chen, L.S., Zheng, J.G., Han, S., Tang, N. and Smith, B.R. (2008) Aluminum-induced effects on photosystem II photochemistry in citrus leaves assessed by the chlorophyll a fluorescence transient. *Tree Physiol.* 28: 1863–1871.

Kanazawa, A. and Kramer, D.M. (2002) In vivo modulation of nonphotochemical exaction quenching (NPQ) by regulation of the chloroplast ATP synthase. *Proc. Natl. Acad. Sci. USA* 99: 12789–12794.

Kern, J., Loll, B., Zouni, A., Saenger, W., Irrgang, K.D. and Biesiadka, J. (2005) Cyanobacterial photosystem II at 3.2 Å resolution—the plastoquinone binding pockets. *Photosynth. Res.* 84: 153–159.

Kim, E.H., Razeghifard, R., Anderson, J.M. and Chow, W.S. (2007) Multiple sites of retardation of electron transfer in photosystem II after hydrolysis of phosphatidylglycerol. *Photosynth. Res.* 93: 149–158.

Kramer, D.M., Johnson, G., Kiirats, O. and Edwards, G.E. (2004) New fluorescence parameters for the determination of Q_A redox state and excitation energy fluxes. *Photosynth. Res.* 79: 209–218.

Li, Q., Xing, D., Jia, L. and Wang, J.S. (2007) Mechanism study on the origin of delayed fluorescence by an analytic modeling of the electronic reflux for photosynthetic electron transport chain. *J. Photochem. Photobiol. B: Biol.* 87: 183–190.

Li, Z. and Xing, D. (2011) Mechanistic study of mitochondria-dependent programmed cell death induced by aluminum phytotoxicity using fluorescence techniques. *J. Exp. Bot.* 62: 331–343.

Lu, C.M., Qiu, N.W., Wang, B.S. and Zhang, J.H. (2003) Salinity treatment shows no effects on photosystem II photochemistry, but increases the resistance of photosystem II to heat stress in halophyte *Suaeda salsa*. *J. Exp. Bot.* 54: 851–860.

Lu, C.M. and Zhang, J.H. (2000) Role of light in the response of PSII photochemistry to salt stress in the cyanobacterium *Spirulina platensis*. *J. Exp. Bot.* 51: 911–917.

Mihailovic, N., Drazic, G. and Vucinic, Z. (2008) Effects of aluminum on photosynthetic performance in Al-sensitive and Al-tolerant maize inbred lines. *Photosynthetica* 46: 476–480.

Moustakas, M., Ouzounidou, G. and Lannoye, R. (1995) Aluminum effects on photosynthesis and elemental uptake in an aluminum-tolerant and nontolerant wheat cultivar. *J. Plant Nutr.* 18: 669–683.

Ono, K., Yamamoto, Y., Hachiya, A. and Matsumoto, H. (1995) Synergistic inhibition of growth by aluminum and iron of tobacco (*Nicotiana tabacum* L.) cells in suspension culture. *Plant Cell Physiol.* 36: 115–125.

Panda, S.K., Yamamoto, Y., Kondo, H. and Matsumoto, H. (2008) Mitochondrial alterations related to programmed cell death in tobacco cells under aluminum stress. *Compt. Rend. Biol.* 311: 597–610.

Petrouleas, V. and Diner, B.A. (1990) Formation by NO of nitrosyl adducts of redox components of the photosystem II reaction center. I: NO binds to the acceptor-side non-heme iron. *Biochim. Biophys. Acta* 1015: 131–140.

Putty-Reddy, S., Denys, P., László, K., Gyõzõ, G. and Murthy, S.D.S. (2005) The effects of salt stress on photosynthetic electron transport and thylakoid membrane proteins in the cyanobacterium *Spirulina platensis*. *J. Biochem. Mol. Biol.* 38: 481–485.

Samuilov, V.D., Lagunova, E.M., Gostimsky, S.A., Timofeev, K.N. and Gusev, M.V. (2003) Role of chloroplast photosystems II and I in apoptosis of pea guard cells. *Biochemistry (Mosc.)* 68: 912–917.

Sanakis, Y., Goussias, C., Mason, R.P. and Petrouleas, V. (1997) NO interacts with the tyrosine radical Y_D of photosystem II to form an iminoxyl radical. *Biochemistry* 36: 1411–1417.

Schreiber, U. (2004) Pulse-amplitude-modulation (PAM) fluorometry and saturation pulse method: an overview. *In* Chlorophyll a fluorescence. A signature of photosynthesis. Edited by Papageorgiou, G. and Govindjee. pp. 279–319. Springer, Dordrecht.

Silva, I.R., Smyth, T.J., Moxley, D.F., Carter, T.E., Allen, N.S. and Rufty, T.W. (2000) Aluminum accumulation at nuclei of cells in the root tip. *Fluorescence detection using Lumogallion and confocal laser scanning microscopy. Plant Physiol.* 123: 543–552.

Simon, H.U., Haj-Yehia, A. and Levi-Schaffer, F. (2000) Role of reactive oxygen species (ROS) in apoptosis induction. *Apoptosis* 5: 415–418.

Tanaka, A. and Tanaka, R. (2006) Chlorophyll metabolism. *Curr. Opin. Plant Biol.* 9: 248–255.

Trtilek, M., Kramer, D.M. and Koblizek, M. (1997) Dual-modulation LED kinetic fluorometer. *J. Luminesc.* 72–74: 597–599.

Van Breusegem, F. and Dat, J.F. (2006) Reactive oxygen species in plant cell death. *Plant Physiol.* 141: 384–390.

Van Heerden, P.D.R., Kruger, G.H.J. and Louw, M.K. (2007) Dynamic responses of photosystem II in the Namib Desert shrub, *Zygophyllum prismatocarpum*, during and after foliar deposition of limestone dust. *Environ. Pollut.* 146: 34–45.

Vitaly, D.S., Elena, M.L., Dmitry, B.K., Elena, V.D., Yana, V.M. and Mikhail, V.G. (2003) Participation of chloroplasts in plant apoptosis. *Biosci. Rep.* 3: 103–117.

Wang, J.S., Xing, D., Zhang, L.R. and Jia, L. (2007) A new principle photosynthesis capacity biosensor based on quantitative measurement of delayed fluorescence in vivo. *Biosens. Bioelectron.* 22: 2861–2868.

Wodala, B., Deak, Z., Vass, I., Erdei, L., Altorjay, I. and Horvath, F. (2008) In vivo target sites of nitric oxide in photosynthetic electron transport as studied by chlorophyll fluorescence in pea leaves. *Plant Physiol.* 146: 1920–1927.

Yamamoto, Y., Kobayashi, Y., Rama, D.S., Sanae, R. and Matsumoto, H. (2002) Aluminum toxicity is associated with mitochondrial dysfunction and the production of reactive oxygen species in plant cells. *Plant Physiol.* 128: 63–72.

Yang, X., Liang, Z., Wen, X. and Lu, C. (2008) Genetic engineering of the biosynthesis of glycinebetaine leads to increased tolerance of photosynthesis to salt stress in transgenic tobacco plants. *Plant Mol. Biol.* 66: 73–86.

Zhang, L.M., Shangguan, Z.P., Mao, M.C. and Yu, G.R. (2003) Effects of long-term application of nitrogen fertilizer on leaf chlorophyll fluorescence of upland winter wheat. *Chin. J. Appl. Eco.* 14: 695–698.

Zhang, L.R. and Xing, D. (2008) Rapid determination of the damage to photosynthesis caused by salt and osmotic stresses using delayed fluorescence of chloroplast. *Photochem. Photobiol. Sci.* 7: 352–360.

Zhao, B.B., Wang, J., Gong, H.M., Wen, X.G., Ren, H.Y. and Lu, C.M. (2008) Effects of heat stress on PSII photochemistry in a cyanobacterium *Spirulina platensis*. *Plant Sci.* 175: 556–564.